Single-Component and Binary Adsorption Equilibria of Fructooligosaccharides, Glucose, Fructose, and Sucrose on a Ca-Form Cation Exchanger

Katarína Vaňková, Michal Gramblička, and Milan Polakovič*

Slovak University of Technology, Faculty of Chemical and Food Technology, Institute of Chemical and Environmental Engineering, Department of Chemical and Biochemical Engineering, Radlinského 9, 812 37 Bratislava, Slovakia

Fructooligosaccharides (1-kestose, 1-nystose, 1^F-fructofuranosylnystose) can be obtained by adsorption separation from their mixtures with fructose, glucose, and sucrose. Fixed-bed adsorption of single saccharides and their binary mixtures on the cation-exchange resin Amberlite CR1320 CA was investigated at the operation temperature of 60 °C and a saccharide concentration range up to 400 $g \cdot L^{-1}$. All adsorption isotherms obtained by frontal chromatography were linear in this range. The distribution coefficients of the saccharides decreased with their molecular weight, which reflected the key role of the size-exclusion effect of the resin. The binary adsorption equilibria showed that the values of the distribution coefficients of all saccharides besides fructose were slightly lower in the presence of another saccharide.

Introduction

Fructooligosaccharides (FOSs) are a specific group of fructan oligomers, which have beneficial effects for human health. FOSs are low-caloric, noncariogenic, and nonmutagenic.[1,2] They have broad application in the food and pharmaceutical industries. FOSs are catalytic products of fructosyltransferase action on sucrose.[3−5] The reaction mixture contains the main product short-chain FOSs, unreacted sucrose, and glucose with fructose as the byproduct. The short-chain FOSs are 1-kestose (GF_2), 1-nystose (GF_3), and 1^F-fructofuranosylnystose (GF_4), in which two, three, and four fructose units are bound to one unit of glucose, respectively.[6] Various chromatographic techniques, which have been applied for separation of different saccharide mixtures,[7−10] could be the best option for the separation of FOSs from the reaction mixture.

Diverse cation-exchange resins are used for saccharide separations in the industry due to their good sorption capacity and selectivity.[11] Sulfonated cross-linked styrene-divinylbenzene cation-exchange resins in Ca^{2+}, Mg^{2+}, Na^+, or K^+ salt forms, which have an ability to withstand osmotic shocks, are considered the best resin types.[8,12] Pb^{2+} and Ag^+ form resins that exhibited excellent properties for the separation of short-chain FOSs in laboratory experiments,[13−15] but they are, of course, not suitable for industrial food applications. The salt form and degree of cross-linking are the most important characteristics of each resin that influence its separation performance. Resins with a higher degree of cross-linking have a lower capacity but higher selectivity and stability.[12] Vente et al. found that the degree of cross-linking had a larger effect on the sorption characteristics than the type of cation.[16] The sorption properties are also affected by water partitioning inside the pores of resin particles and a hydration shell around the cation functional groups.[16] Other important properties of suitable resins are nontoxicity, low cost, and mechanical, chemical, and biological stability, which prolong the lifetime.

* Corresponding author. E-mail: milan.polakovic@stuba.sk. Phone: +421-2-59325254. Fax: +421-2-52496920.

Several key mechanisms are utilized in separation of oligosaccharides from mono- and disaccharides such as size exclusion, steric effect (pore blocking), and complex formation with resin functional groups. The interplay of these mechanisms causes a complex adsorption behavior of the saccharide mixtures. Size exclusion is the main separation mechanism when the resin pore diameter is close to the diameter of the separated molecules. FOSs as relatively large molecules are then more or less excluded from most pores. The relation between the saccharide type and charge density or hydration number of the cation was studied by Morel et al.[11] They found that complex formation is more significant in the separation of molecules of the same size but different structure such as glucose and fructose.

Experimentally determined adsorption isotherms of FOSs and impurity saccharides[17−19] represent essential data for the design and optimization of chromatographic separation processes. There are numerous methods for the determination of adsorption isotherms, which are analyzed and reviewed in several articles.[20,21] Linear adsorption isotherms of saccharides on cation-exchange resins were observed for concentrations up to 400 $g \cdot L^{-1}$ in most cases[16−18,22,23] when a visible departure from the linearity occurred above this value.[18,24] This effect has been explained by the dependence of resin swelling pressure on saccharide concentration that caused its shrinking and simultaneous decrease of water pore content.[25,26]

In our previous publication, we used a static method for the determination of single-component isotherms of saccharides and multicomponent isotherms of FOSs for a commercial mixture on four different commercial ion exchangers.[17] The main objective of this study was to determine the single-component adsorption isotherms of pure FOSs and binary adsorption isotherms of key saccharides for the efficiency of chromatographic separation. A Ca^{2+}-based resin was used, which was found to be the best in previous work.[17] The operation temperature was 60 °C since it is a good compromise between the reduction of viscosity and preservation of carbohydrates.[18] Frontal analysis was chosen because it is a much less laborious method for binary adsorption measurement.[27] Since some authors reported differences in the equilibrium data for saccha-

10.1021/je9003965 CCC: $40.75
Published on Web 09/02/2009

ride adsorption obtained by different measurement methods,[20,21] the single-component isotherms of monosaccharides and sucrose previously determined by the static method were re-examined by frontal analysis in this study.

Experimental Section

Materials. The resin used was Amberlite CR1320Ca (Rohm and Haas, Paris, France) with the $(SO_3^-)_2Ca^{2+}$ functional group. The particle diameter and ion-exchange capacity were 320 μm and 1.63 equiv·L^{-1}, respectively. Fructose (F), glucose (G), and sucrose (GF) were obtained from Microchem (Pezinok, Slovakia). 1-Kestose (GF_2), 1-nystose (GF_3), and 1^F-fructofuranosylnystose (GF_4) were products of Wako Pure Chemical Industries (Osaka, Japan). Water, which was used to prepare saccharide solutions and eluent, was double distilled and filtered through a 0.2 μm cellulose−nitrate filter. All other chemicals were of analytical grade and were obtained from readily available commercial sources.

Methods. The resin Amberlite CR1320Ca was washed several times with double distilled water and was separated on a sintered-glass filter. The water content of the resin was determined by drying wet particles at 80 °C until constant weight was reached. The value of water mass fraction was 48.3 % with a standard deviation of 0.7 %.

A glass column Superformance 150-16 (Götec Labor Technik, Muhltal, Germany) was packed with the resin slurry. The column volume V_C was 23.0 mL. The column hold-up volume V_0 was measured using Dextran 2000000 (Polymer Standard Service, Mainz Germany), which did not diffuse into the resin particle pores. The concentration of the dextran was 0.8 kg·m^{-3}. The column bed voidage, $\varepsilon = V_0/V_C$, was 0.384 with a standard deviation of 0.009. No visual change of bed volume was observed during the experiments.

Adsorption isotherms were determined for all single saccharides and six binary mixtures using the staircase method of frontal analysis. The column was first equilibrated with pure eluent (water). For single-component adsorption, the saccharide inlet concentration was stepwise increased up to 100 g·L^{-1} or 400 g·L^{-1}, respectively. For binary adsorption, the total saccharide concentration in the feed was in all steps 400 g·L^{-1}, but the proportion of the individual components was varied. To obtain adsorption and desorption data for both components, the concentration of one component was first stepwise increased from (0 to 400) g·L^{-1} and then decreased in the reverse direction.

Saccharide solutions or eluent water were pumped by two peristaltic pumps (Gilson, Middleton, WI) through a six-port switching valve (Knauer, Berlin, Germany) at a flow rate of 1 cm^3·min^{-1}. The inlet pH of sucrose and FOS solutions was adjusted to 8.5 with 0.5 M $Ca(OH)_2$. The column was thermostatted at 60 °C by means of JetStream Plus II (Thermotechnic Products, Langenzersdorf, Austria). The column outlet solution was monitored by a refractive index (RI) detector (Knauer, Berlin, Germany) and was distributed into 0.5 mL fractions using the fraction-collector Frac-920 (GE Healthcare, NY, USA). All concentrations were determined by HPLC (Knauer, Berlin, Germany) using the column REZEX RSO-Oligosaccharide (Ag^+ form, 200 × 10 mm, Phenomenex, Torrance, CA). The column temperature was maintained at 40 °C by the Jetstream Plus II thermostat. Redistilled water was used as the mobile phase at a flow rate of 0.3 cm^3·min^{-1}. The amount injected by an autosampler (Gilson, Middleton, WI) was 10 μL when saccharide detection was performed by a differential flow refractometer at 25 °C.

The equilibrium solid-phase concentration (related to the mass of dry adsorbent) q_i in the ith adsorption step for the inlet liquid-phase concentration c_{0i} was calculated from the equation

$$q_i = q_{i-1} + \frac{A_i\dot{V} - \varepsilon c_{0i}V_C}{(1-\varepsilon)V_C\rho_c} \quad (1)$$

where $\dot{V}$ is the flow rate; ρ_c is the resin density; t_D is the extra-column dead time; and A_i is the integral obtained from the experimental breakthrough curve $c_i(t)$

$$A_i = \int_{t_{i-1}}^{t_i} [c_{0i} - c_i(t)]dt - c_{0i}t_D \quad (2)$$

Numerical integration was carried out using the software Matlab R2006 (The MathWorks, Massachusetts, USA). For desorption steps, analogous equations were used

$$q_i = q_{i-1} - \frac{A_i\dot{V} - \varepsilon c_{0i}V_C}{(1-\varepsilon)V_C\rho_c} \quad (3)$$

$$A_i = \int_{t_{i-1}}^{t_i} [c_i(t) - c_{0i}]dt - c_{0i}t_D \quad (4)$$

Results and Discussion

Table 1 presents the results of single-component adsorption of saccharides on Amberlite (TM) CR1320 CA at 60 °C. The equilibrium data obtained by frontal analysis were in the concentration range (0 to 400) g·L^{-1} for fructose, glucose, sucrose, and 1-kestose, whereas for 1-nystose and 1^F-fructofuranosylnystose, the upper concentration limit was 100 g·L^{-1}. It is evident from Table 1 that the adsorbed amount decreased from fructose to 1^F-fructofuranosylnystose. The dependencies between the equilibrium solid-phase and liquid-phase concentrations, q and c, were linear for all components as illustrated in Figure 1. They could thus be characterized by a single parameter, the distribution coefficient, K, which was the slope of the linear least-squares fit of the experimental data.

Table 2 presents the distribution coefficients of saccharides for single-component adsorption which were in the range from 0.171 dm^3·kg^{-1} for 1^F-fructofuranosylnystose to 0.762 dm^3·kg^{-1} for fructose. The standard deviations of K of the fitted data did not exceed the value of 0.002 dm^3·kg^{-1}, which corresponded to a relative error of K from 0.3 % to 1.2 %. The values of K for fructose and sucrose obtained here differed by 0.5 % and 1.1 %, respectively, from those obtained by the static method.[17] The corresponding difference for glucose was 13.1 % when a smaller value was obtained previously. For this reason, the experiment was repeated, and the value of 0.597 dm^3·kg^{-1} was confirmed. The single-component distribution coefficients of 1-kestose, 1-nystose, and 1^F-fructofuranosylnystose can be compared only with the results obtained for a commercial multicomponent mixture.[17] The values obtained previously were 13.3 %, 16.1 %, and 16.3 % smaller, respectively. These differences can be reasonably explained by the effect of influencing of adsorption by other saccharides in the mixture as discussed below.

The distributions coefficients of the saccharides decreased with their molecular weight, i.e. in the order fructose > glucose > sucrose > 1-kestose > 1-nystose > 1^F-fructofuranosylnystose. This order and low values of distribution coefficients reflect a dominating role of the size-exclusion effect of the resin in adsorption of the saccharides. A value of the distribution coefficient of fructose 0.762, which was 27.6 % larger than that of glucose, implies that the size-exclusion effect was not the single mechanism responsible for fructose adsorption. Formation of a complex by ion−dipole interactions of hydroxyl groups of

Table 1. Single-Component Adsorption Equilibrium Data

fructose (M = 180 g·mol^{-1})		glucose (M = 180 g·mol^{-1})		sucrose (M = 342 g·mol^{-1})		1-kestose (M = 504 g·mol^{-1})		1-nystose (M = 667 g·mol^{-1})		1^F-fructofuranosylnystose (M = 829 g·mol^{-1})	
c g·L^{-1}	q g·kg^{-1}	c g·L^{-1}	q g·kg^{-1}	c g·L^{-1}	q g·kg^{-1}	c g·L^{-1}	q g·kg^{-1}	c g·L^{-1}	q g·kg^{-1}	c g·L^{-1}	q g·kg^{-1}
6.1	4.6	7.5	5.0	6.1	2.5	12.0	3.3	6.0	1.2	8.9	1.4
12.4	9.4	15.0	9.3	12.2	5.2	17.9	5.0	12.0	2.5	17.8	2.9
18.6	14.2	22.4	13.7	18.3	7.8	23.6	6.7	18.0	3.9	26.7	4.3
24.7	19.0	29.9	18.2	36.5	15.7	36.0	9.7	24.0	5.2	35.6	5.7
37.1	28.0	44.9	26.5	48.7	21.0	41.7	11.6	36.0	7.9	53.4	8.5
74.2	56.7	59.8	34.8	73.0	30.8	48.0	13.4	48.0	10.7	71.2	12.0
99.5	74.4	89.7	54.1	101.0	45.0	55.0	15.6	72.1	16.4	91.7	15.6
117.8	88.1	129.8	78.7	143.8	61.0	79.0	22.0	96.1	21.5	106.7	18.8
132.7	99.0	164.9	99.6	173.8	75.7	101.0	28.2				
147.8	111.1	192.9	117.7	204.4	87.0	124.5	35.0				
157.4	122.7	223.9	133.3	228.4	97.1	153.0	42.6				
179.0	138.4	292.8	175.6	257.7	108.8	182.5	51.0				
198.8	151.5	374.4	221.1	288.3	122.1	247.5	67.5				
243.8	184.9			330.4	140.4	284.0	80.0				
293.7	223.8					357.5	100.0				
342.9	262.2										
393.4	299.8										
Standard Deviation Value of q/g·kg^{-1}											
1.254		1.206		0.839		0.402		0.169		0.374	

Table 2. Distribution Coefficients[a] of Single-Component Isotherms

saccharide	K/dm^3·kg^{-1}
fructose	0.762 ± 0.002
glucose	0.597 ± 0.002
sucrose	0.426 ± 0.002
1-kestose	0.277 ± 0.001
1-nystose	0.224 ± 0.001
1^F-fructofuranosylnystose	0.171 ± 0.002

[a] The value after the ± sign gives the standard deviation.

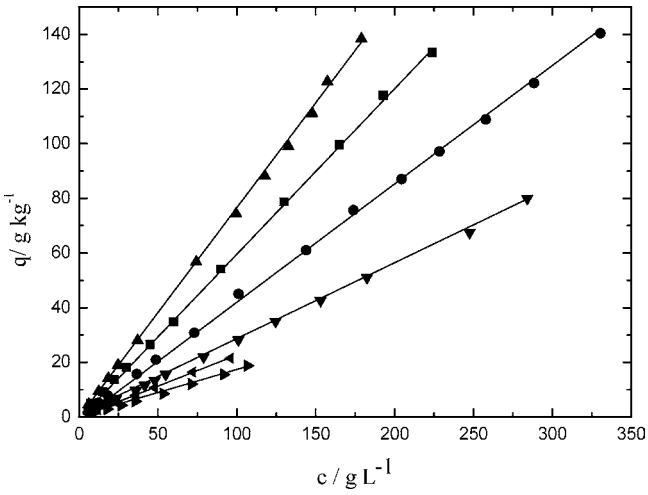

Figure 1. Single-component adsorption isotherms of ▲, fructose; ■, glucose; ●, sucrose; ▼, kestose; solid triangle pointing left, nystose; and solid triangle pointing right, 1^F-fructofuranosylnystose on Amberlite CR1320Ca at 60 °C. The lines are the fits with the linear adsorption isotherm.

this furanose-form ketose with the water molecules of the hydration shell of Ca^{2+} functional groups of the resin could be assumed.[28] The relative difference between the distribution coefficients of fructose and glucose corresponds to the fraction of bound nonfreezable pore-water of polystyrene−divinylbenzene resins.[29] Since the adsorption isotherm is linear over a large concentration range, it is therefore reasonable to assume that fructose partitions both in the bound nonfreezable pore-water and in the freezable pore-water, whereas glucose and other saccharides partition mostly only in the freezable pore-water.

As has been mentioned in the Experimental Section, binary adsorption isotherms were determined for the mixtures of fructose, glucose, sucrose, and 1-kestose having the same total saccharide concentration of 400 g·L^{-1}. Tables 3 to 8 give equilibrium data for all six combinations of binary mixtures obtained from adsorption fronts and Tables 9 to 14 those from desorption fronts. It should be mentioned that adsorption and desorption fronts were obtained simultaneously because one of the saccharides was adsorbed and the second one was desorbed.

Table 3. Binary Adsorption Equilibrium Data of Fructose and Sucrose Obtained from Adsorption Fronts

fructose		sucrose	
c/g·L^{-1}	q/g·kg^{-1}	c/g·L^{-1}	q/g·kg^{-1}
9.6	8.0	13.9	5.0
19.1	15.3	27.8	11.3
28.5	22.9	41.5	16.5
38.1	29.4	55.5	22.7
47.8	35.6	69.5	27.8
95.0	72.5	138.5	56.0
114.5	85.5	139.0	57.5
153.0	116.0	167.0	67.0
191.0	144.5	208.5	80.5
229.0	175.5	222.5	84.0
280.5	213.5	250.5	94.5
325.5	251.0	278.5	107.0
381.0	286.5	334.0	129.0
Standard Deviation Value of q/g·kg^{-1}			
1.609		1.807	

Table 4. Binary Adsorption Equilibrium Data of Fructose and Glucose Obtained from Adsorption Fronts

fructose		glucose	
c/g·L^{-1}	q/g·kg^{-1}	c/g·L^{-1}	q/g·kg^{-1}
8.0	3.2	6.0	2.4
16.0	10.4	11.9	5.0
24.0	16.7	17.9	9.3
32.0	22.8	23.8	12.2
48.1	35.1	35.7	18.0
79.0	58.5	47.6	24.1
95.5	70.0	71.0	37.1
128.0	93.0	119.0	63.5
160.0	117.0	143.0	76.0
192.0	143.5	190.5	100.0
256.5	197.0	238.0	130.0
320.5	246.5	286.0	153.5
384.5	295.0	367.5	196.5
Standard Deviation Value of q/g·kg^{-1}			
2.787		1.236	

Table 5. Binary Adsorption Equilibrium Data of Fructose and 1-Kestose Obtained from Adsorption Fronts

fructose		1-kestose	
c/g·L^{-1}	q/g·kg^{-1}	c/g·L^{-1}	q/g·kg^{-1}
6.3	4.4	5.7	1.5
18.9	15.2	11.4	3.1
24.9	17.8	22.9	6.3
37.4	29.1	34.3	9.0
71.5	55.0	45.8	12.4
99.0	73.5	68.8	17.9
124.0	96.5	109.9	28.8
158.5	117.0	132.2	34.3
187.0	139.5	164.9	42.6
244.0	184.0	185.2	48.2
297.0	227.5	252.9	67.6
347.5	265.5	277.4	74.4
398.5	304.5	369.7	99.0
Standard Deviation Value of q/g·kg^{-1}			
1.813		0.634	

Table 6. Binary Adsorption Equilibrium Data of Glucose and Sucrose Obtained from Adsorption Fronts

glucose		sucrose	
c/g·L^{-1}	q/g·kg^{-1}	c/g·L^{-1}	q/g·kg^{-1}
6.6	3.8	13.9	4.6
13.1	7.0	20.7	6.6
19.5	10.8	27.8	9.3
26.2	14.5	41.7	13.9
39.4	22.3	55.7	18.7
52.5	28.2	83.5	29.1
78.7	43.6	139.1	49.7
131.2	73.5	173.3	59.5
145.2	82.1	214.4	74.8
189.8	104.8	234.4	82.8
240.4	132.7	259.4	90.4
284.5	158.5	278.3	97.6
372.9	208.3	332.7	117.1
Standard Deviation Value of q/g·kg^{-1}			
0.680		0.661	

Table 7. Binary Adsorption Equilibrium Data of Glucose and 1-Kestose Obtained from Adsorption Fronts

glucose		1-kestose	
c/g·L^{-1}	q/g·kg^{-1}	c/g·L^{-1}	q/g·kg^{-1}
6.2	3.2	4.7	1.5
13.3	6.5	9.8	2.7
19.4	10.4	22.0	6.0
22.3	13.1	35.2	8.9
38.3	20.0	47.0	11.9
45.8	25.3	80.2	20.5
85.8	47.6	109.7	27.6
123.3	68.6	134.9	34.2
153.8	84.9	169.4	42.9
188.9	108.0	187.9	47.7
231.7	134.0	234.9	60.9
292.3	167.3	289.2	73.8
370.3	211.0	368.9	95.5
Standard Deviation Value of q/g·kg^{-1}			
1.367		0.473	

Table 8. Binary Adsorption Equilibrium Data of Sucrose and 1-Kestose Obtained from Adsorption Fronts

sucrose		1-kestose	
c/g·L^{-1}	q/g·kg^{-1}	c/g·L^{-1}	q/g·kg^{-1}
14.3	4.3	7.9	1.2
29.4	8.6	11.9	3.0
41.9	12.7	29.4	6.4
57.9	16.9	39.4	7.8
75.4	22.7	52.5	11.9
114.4	35.1	79.9	18.4
147.3	44.3	107.5	23.8
174.4	53.0	134.5	30.8
208.7	63.2	156.9	35.5
228.8	68.7	189.3	42.3
259.4	78.1	229.4	51.8
282.3	85.4	269.9	61.5
328.9	100.0	352.4	80.5
Standard Deviation Value of q/g·kg^{-1}			
0.360		0.498	

Table 9. Binary Adsorption Equilibrium Data of Fructose and Sucrose Obtained from Desorption Fronts

fructose		sucrose	
c/g·L^{-1}	q/g·kg^{-1}	c/g·L^{-1}	q/g·kg^{-1}
9.6	7.9	13.9	5.2
19.1	15.4	27.8	11.4
28.5	22.70	41.5	16.8
38.1	29.5	55.5	22.4
47.8	35.5	69.5	27.5
95.0	72.4	138.5	56.1
114.5	85.3	139.0	57.0
153.0	115.8	167.0	66.8
191.0	144.6	208.5	80.2
229.0	176	222.5	83.6
280.5	213.8	250.5	94.0
325.5	250.8	278.5	108.0
381.0	286.3	334.0	128.0
Standard Deviation Value of q/g·kg^{-1}			
1.664		1.821	

Table 10. Binary Adsorption Equilibrium Data of Fructose and Glucose Obtained from Desorption Fronts

fructose		glucose	
c/g·L^{-1}	q/g·kg^{-1}	c/g·L^{-1}	q/g·kg^{-1}
8.0	2.9	6.0	2.5
16.0	11.2	11.9	5.4
24.0	17.3	17.9	10.4
32.0	23.1	23.8	12.1
48.1	35.6	35.7	18.4
79.0	59.2	47.6	24.7
95.5	70.7	71.0	37.9
128.0	94.1	119.0	64.2
160.0	118.4	143.0	76.3
192.0	145.1	190.5	100.8
256.5	198.2	238.0	130.2
320.5	245.3	286.0	152.9
384.5	293.0	367.5	196.3
Standard Deviation Value of q/g·kg^{-1}			
2.115		1.053	

Figures 2 and 3 illustrate the results of binary adsorption of fructose and sucrose, respectively, in the presence of the other three saccharides and their comparison with single-component adsorption. The figures show that the linear character of the dependence between the solid- and liquid-phase concentrations of a component was not affected by the presence of another component. This was true for all binary adsorption equilibria (Tables 15 to 18).

The distribution coefficients of all saccharides for binary adsorption were determined separately from adsorption front (K_{ads}) and desorption front (K_{des}) equilibrium and also from all data (K), and they are presented in Tables 15 to 18. It is evident that identical values were obtained from both types of frontal analysis data. The standard deviations of the distribution coefficients for binary adsorption were the same as for single-component adsorption in the case of glucose (Table 16) and kestose (Table 18). They were somewhat higher in the case of fructose (Table 15) and sucrose (Table 17), but in relative values, they did not exceed 0.5 % and 1 %, respectively.

A key observation was that the distribution coefficient of fructose was not affected by the presence of another saccharide

Table 11. Binary Adsorption Equilibrium Data of Fructose and 1-Kestose Obtained from Desorption Fronts

fructose		1-kestose	
c/g·L^{-1}	q/g·kg^{-1}	c/g·L^{-1}	q/g·kg^{-1}
6.3	4.1	5.7	1.8
18.9	14.9	11.4	3.5
24.9	18.2	22.9	6.2
37.4	29.7	34.3	8.5
71.5	53.9	45.8	12.9
99.0	73.4	68.8	17.3
124.0	97.1	109.9	29.1
158.5	116.7	132.2	35.2
187.0	140.1	164.9	42.5
244.0	183.8	185.2	48.7
297.0	227.1	252.9	67.9
347.5	264.8	277.4	75.1
398.5	305.2	369.7	98.6
Standard Deviation Value of q/g·kg^{-1}			
1.896		0.733	

Table 12. Binary Adsorption Equilibrium Data of Glucose and Sucrose Obtained from Desorption Fronts

glucose		sucrose	
c/g·L^{-1}	q/g·kg^{-1}	c/g·L^{-1}	q/g·kg^{-1}
6.6	4.0	13.9	5.0
13.1	6.5	20.7	6.3
19.5	10.5	27.8	9.0
26.2	14.8	41.7	13.7
39.4	22.1	55.7	19.0
52.5	28.0	83.5	29.5
78.7	44.0	139.1	49.5
131.2	73.1	173.3	60.0
145.2	82.3	214.4	74.2
189.8	104.2	234.4	82.4
240.4	132.6	259.4	90.6
284.5	159.0	278.3	97.2
372.9	208.7	332.7	117.5
Standard Deviation Value of q/g·kg^{-1}			
0.904		0.688	

Table 13. Binary Adsorption Equilibrium Data of Glucose and 1-Kestose Obtained from Desorption Fronts

glucose		1-kestose	
c/g·L^{-1}	q/g·kg^{-1}	c/g·L^{-1}	q/g·kg^{-1}
6.2	3.4	4.7	1.4
13.3	6.8	9.8	2.6
19.4	10.3	22.0	5.8
22.3	12.9	35.2	9.1
38.3	21.3	47.0	11.8
45.8	26.1	80.2	20.6
85.8	46.8	109.7	28.1
123.3	68.1	134.9	33.7
153.8	85.3	169.4	43.3
188.9	107.5	187.9	48.2
231.7	133.7	234.9	61.3
292.3	166.8	289.2	72.8
370.3	212.2	368.9	96.1
Standard Deviation Value of q/g·kg^{-1}			
1.301		0.708	

(Figure 2 and Table 15), whereas the distribution coefficients of glucose, sucrose, and 1-kestose for adsorption of binary mixtures were always slightly lower than the corresponding values for single-component adsorption (Figure 3 and Tables 16 to 18). These results are compatible also with those of our previous study when the distribution coefficients of FOSs in a commercial mixture Actilight 950P (Beghin Meiji, NeuillySur Seine, France) are lower than the corresponding single-component distribution coefficients in Table 1. The partitioning of fructose in the bound pore-water was thus not affected by

Table 14. Binary Adsorption Equilibrium Data of Sucrose and 1-Kestose Obtained from Desorption Fronts

sucrose		1-kestose	
c/g·L^{-1}	q/g·kg^{-1}	c/g·L^{-1}	q/g·kg^{-1}
14.3	4.7	7.9	1.6
29.4	8.3	11.9	3.1
41.9	12.4	29.4	6.7
57.9	17.3	39.4	8.3
75.4	23.0	52.5	12.2
114.4	34.8	79.9	18.6
147.3	44.7	107.5	23.5
174.4	52.9	134.5	30.7
208.7	63.6	156.9	35.6
228.8	69.2	189.3	42.8
259.4	78.7	229.4	51.2
282.3	84.6	269.9	61.9
328.9	98.9	352.4	80.7
Standard Deviation Value of q/g·kg^{-1}			
0.395		0.531	

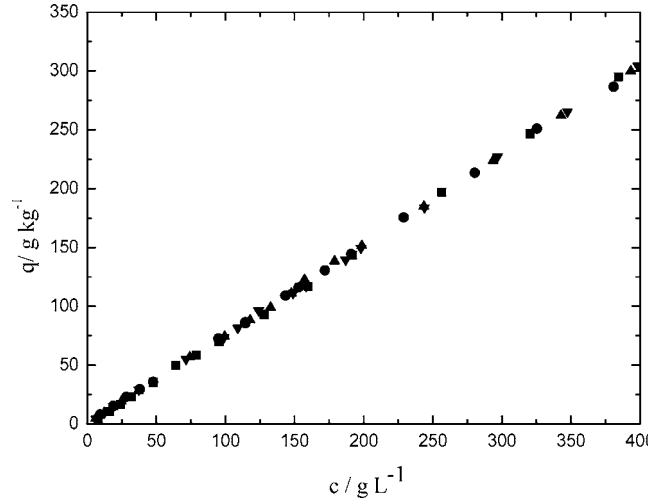

Figure 2. Adsorption isotherms of fructose on Amberlite CR 1320 Ca at 60 °C. ▲, single-component and binary adsorption in the presence of ■, glucose; ●, sucrose; and ▼, 1-kestose.

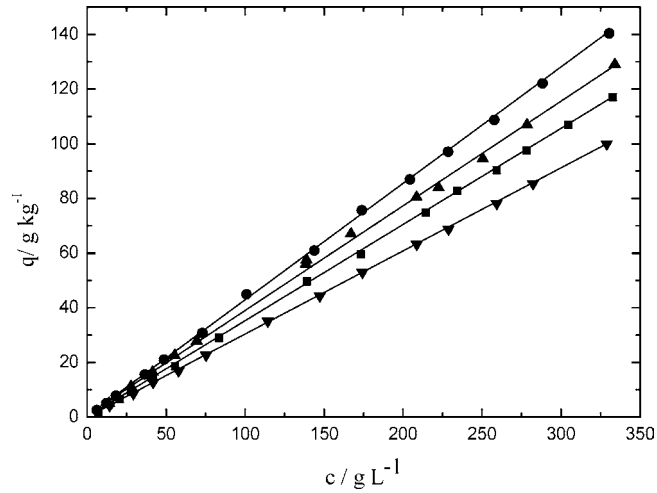

Figure 3. Adsorption isotherms of sucrose on Amberlite CR 1320 Ca at 60 °C. ●, single-component and binary adsorption in the presence of ■, glucose; ▲, fructose; and ▼, 1-kestose. The lines are the fits with the linear adsorption isotherm.

the molecules of glucose, sucrose, and 1-kestose, whereas the partitioning of other saccharides was slightly affected.[30] This may be caused by thermodynamically nonideal behavior of concentrated aqueous solutions of saccharides and complex water structure in the cross-linked resin.

Table 15. Distribution Coefficients[a] of Fructose in Binary Mixtures

	glucose	sucrose	1-kestose
K_{ads}/dm^3·kg^{-1}	0.761 ± 0.004	0.760 ± 0.002	0.761 ± 0.003
K_{des}/dm^3·kg^{-1}	0.761 ± 0.003	0.760 ± 0.002	0.761 ± 0.003
K/dm^3·kg^{-1}	0.761 ± 0.003	0.760 ± 0.002	0.761 ± 0.002

[a] The value after the ± sign gives the standard deviation.

Table 16. Distribution Coefficients[a] of Glucose in Binary Mixtures

	fructose	sucrose	1-kestose
K_{ads}/dm^3·kg^{-1}	0.535 ± 0.002	0.557 ± 0.001	0.569 ± 0.002
K_{des}/dm^3·kg^{-1}	0.536 ± 0.002	0.557 ± 0.002	0.570 ± 0.002
K/dm^3·kg^{-1}	0.535 ± 0.001	0.557 ± 0.001	0.570 ± 0.002

[a] The value after the ± sign gives the standard deviation.

Table 17. Distribution Coefficients[a] of Sucrose in Binary Mixtures

	fructose	glucose	1-kestose
K_{ads}/dm^3·kg^{-1}	0.387 ± 0.003	0.350 ± 0.001	0.303 ± 0.001
K_{des}/dm^3·kg^{-1}	0.386 ± 0.003	0.350 ± 0.001	0.302 ± 0.001
K/dm^3·kg^{-1}	0.386 ± 0.002	0.350 ± 0.001	0.302 ± 0.000

[a] The value after the ± sign gives the standard deviation.

Table 18. Distribution Coefficients[a] of 1-Kestose in Binary Mixtures

	fructose	glucose	sucrose
K_{ads}/dm^3·kg^{-1}	0.266 ± 0.001	0.257 ± 0.001	0.227 ± 0.001
K_{des}/dm^3·kg^{-1}	0.267 ± 0.001	0.257 ± 0.001	0.227 ± 0.001
K/dm^3·kg^{-1}	0.266 ± 0.001	0.257 ± 0.001	0.227 ± 0.001

[a] The value after the ± sign gives the standard deviation.

Conclusions

Frontal analysis of column chromatography was used to determine single-component and binary adsorption equilibria of saccharides pertinent to the separation of product mixtures of an enzymatic conversion of sucrose to fructooligosaccharides by fructosyltransferase. An excellent agreement was found between the values obtained from adsorption and desorption fronts for binary adsorption. The size-exclusion effect thus plays a dominant role in the separation of these saccharides on the calcium-form ion exchanger employed in this study. It was inferred from the differences between the distribution coefficients of fructose and glucose that a complexation effect plays some role in the partitioning of saccharides. It was speculated that the complexation effect is related to different forms of pore water in this microporous resin when, besides ordinary free water, two types of bound water exist in narrow pores, freezable and unfreezable, tightly bound to the polymer backbone. This complex water structure may have been responsible for slight negative saccharide−saccharide interaction effects in binary adsorption of all saccharides but fructose.

Literature Cited

(1) Crittenden, R. G.; Playne, M. J. Production, properties and applications of food-grade oligosaccharides. *Trends Food Sci. Technol.* **1996**, *7*, 353–361.

(2) Yun, J. W. Fructooligosaccharides-occurrence, preparation, and application. *Enzyme Microb. Techol.* **1996**, *19*, 107–117.

(3) Sangeetha, P. T.; Ramesh, M. N.; Prapulla, S. G. Fructooligosaccharide production using fructosyl transferase obtained from recycling culture of *Aspergillus oryzae* CFR 202. *Process Biochem.* **2005**, *40*, 1085–1088.

(4) Duan, K. J.; Chen, J. S.; Sheu, D. C. Kinetic studies and mathematical model for enzymatic production of fructooligosaccharides from sucrose. *Enzyme Microb. Technol.* **1994**, *16*, 334–339.

(5) Yun, J. W.; Song, S. K. The production of high-content fructooligosaccharides from sucrose by the mixed-enzyme system of fructosyltransferase and glucose oxidase. *Biotechnol. Lett.* **1993**, *15*, 573–576.

(6) Csanádi, Z.; Sisak, C. Immobilization of pectinex ultra sp-l pectinase and its application to production of fructooligosaccharides. *Acta Aliment.* **2006**, *35*, 205–212.

(7) Feste, A. S.; Khan, I. Separation of glucooligosaccharides and polysaccharide hydrolysates by gradient elution hydrophilic interaction chromatography with pulsed amperometric detection. *J. Chromatogr. A* **1993**, *630*, 129–139.

(8) Takahashi, Y.; Goto, S. Continuous separation of fructooligosaccharides using an annular chromatography. *Sep. Sci. Technol.* **1994**, *29*, 1311–1318.

(9) Coelho, M. S.; Azevedo, D. C. S.; Teixeira, J. A.; Rodrigues, A. Dextran and fructose separation on an SMB continuous chromatographic unit. *Biochem. Eng. J.* **2002**, *12*, 215–221.

(10) Lin, S. C.; Lee, W. C. Separation of a fructo-oligosaccharide mixture by hydrophilic interaction chromatography using silica-based micropellicular sorbents. *J. Chromatogr. A* **1998**, *803*, 302–306.

(11) Morel-Desrosiers, N.; Morel, J. P. Interaction between cation and sugar. Part 5. Enthalphy and enthropy of interaction of the calcium ion with some aldopentoses and aldohexoses in water at 298.15 K. *J. Chem. Soc.* **1989**, *85*, 3461–3469.

(12) Adachi, S.; Watanabe, T.; Kohashi, M. Effects of the divinylbenzene content and ionic form of cation-exchange resin on the chromatographic separation of maltooligosaccharides. *Agric. Biol. Chem.* **1989**, *53*, 3193–3201.

(13) Antošová, M.; Polakovič, M.; Báleš, V. Separation of fructooligosaccharides on a cation-exchange HPLC column in silver form with refractometric detection. *Biotechnol. Technol.* **1999**, *13*, 889–892.

(14) Van Riel, J. A. M.; Olieman, C. High-performance liquid chromatography of sugars on a mixed cation-exchange resin column. *J. Chromatogr.* **1986**, *362*, 235–242.

(15) Vandáková, M.; Platková, Z.; Antošová, M.; Báleš, V.; Polakovič, M. Optimisation of cultivation conditions for production of fructosyltransferase by *Aureobasidium pullulans*. *Chem. Pap.* **2004**, *58*, 15–22.

(16) Vente, J. A. Adsorbent functionality in relation to selectivity and capacity in oligosaccharide separations. PhD. Thesis, University of Twente, Netherland, 2005.

(17) Gramblièka, M.; Polakoviè, M. Adsorption equilibria of glucose, fructose, sucrose, and fructooligosaccharides on cation exchange resin. *J. Chem. Eng. Data* **2007**, *52*, 345–350.

(18) Nowak, J.; Gedicke, K.; Antos, D.; Piatkowski, W.; Seidel-Morgenstern, A. Synergistic effects in competitive adsorption of carbohydrates on an ion-exchange resin. *J. Chromatogr. A* **2007**, *1164*, 224–234.

(19) Lisec, O.; Hugo, P.; Seidel-Morgenstern, A. Frontal analysis method to determine competitive adsorption isotherms. *J. Chromatogr. A* **2001**, *908*, 19–34.

(20) Vente, J. A.; Bosch, H.; de Haan, A. B.; Bussmann, P. J. T. Evaluation of sugar sorption isotherm measurement by frontal analysis under industrial processing conditions. *J. Chromatogr. A* **2005**, *1066*, 71–79.

(21) Nicoud, R.-M.; Seidel-Morgenstern, A. Adsorption isotherms: experimental determination and application to preparative chromatography. *Isol. Purif.* **1996**, *2*, 165–200.

(22) Azevedo, D. C. S.; Rodrigues, A. E. Obtainment of high-fructose solutions from cashew (Anacardium occidentale, L.) apple juice by SMB chromatography. *Sep. Sci. Technol.* **2000**, *35*, 2561–2581.

(23) Bart, H. J.; Messenbock, R. C.; Byers, C. H.; Prior, A.; Wolfgang, J. Continuous chromatographic separation of fructose, mannitol and sorbitol. *Chem. Eng. Process.* **1996**, *35*, 459–471.

(24) Ching, C. B.; Ho, C.; Hidajat, K.; Ruthven, D. M. Experimental study of a simulated counter-current adsorption system - V Comparison of resin and zeolite adsorbents for fructose-glucose separation at high concentration. *Chem. Eng. Sci.* **1987**, *42*, 2547–2555.

(25) Shioda, K. Chromatographic separation processes. In *Starch Hydrolysis Products*; Worldwide Technology, Production, and Applications: New York, 1992.

(26) Adachi, S.; Mizuno, T.; Matsuno, R. Concentration dependence of the distribution coefficient of maltooligosacharides on a cation-exchange resin. *J. Chromatogr. A* **1995**, *708*, 177–183.

(27) Seidel-Morgenstern, A. Experimental determination of single solute and competitive adsorption isotherms. *J. Chromatogr. A* **2004**, *1037*, 255.

(28) Glueckauf, E., III. The hydration of cations in polystyrene sulphonates. *Proc. R. Soc. London* **1955**, *228*, 322–341.

(29) Baba, T.; Shibukawa, M.; Heya, T.; Abe, S. I.; Oguma, K. Liquid chromatography and differential scanning calorimetry studies on the states of water in polystyrene-divinylbenzene copolymer gels. *J. Chromatogr. A* **2003**, *1010*, 177–184.

(30) Altenhoner, U.; Meurer, M.; Strube, J.; Schmidt-Traub, H. Parameter estimation for the simulation of liquid chromatography. *J. Chromatogr. A* **1997**, *769*, 59–69.

Received for review May 4, 2009. Accepted August 21, 2009. This study was supported by Science and Technology Assistance Agency APVV (LPP-0234−06).

JE9003965